

# A comparison of shortwave reflectance over the East Antarctic Plateau observed by CERES to that estimated from surface reflectance observations

Stephen R. Hudson,<sup>1</sup> Stephen G. Warren,<sup>2</sup> and Seiji Kato<sup>3</sup>

Received 21 January 2010; revised 9 April 2010; accepted 20 April 2010; published 22 October 2010.

[1] Spectral albedo and bidirectional reflectance of snow were measured at Dome C on the East Antarctic Plateau for wavelengths of 350–2400 nm and solar zenith angles of 52°–87°. A parameterization of bidirectional reflectance, based on those measurements, is used as the lower boundary condition in the atmospheric radiation model SBDART to calculate radiance and flux at the top of the atmosphere (TOA). The model’s atmospheric profile is based on radiosoundings at Dome C and ozonesoundings at the South Pole. Computed TOA radiances are integrated over wavelength for comparison with the Clouds and the Earth’s Radiant Energy System (CERES) shortwave channel. CERES radiance observations and flux estimates from four clear days in January 2004 and January 2005 from within 200 km of Dome C are compared with the TOA radiances and fluxes computed for the same solar zenith angle and viewing geometry, providing 11,000 comparisons. The measured radiance and flux are lower than the computed values. The median difference is about 7% for CERES on Terra, and 9% on Aqua. Sources of uncertainty in the model and observations are examined in detail and suggest that the measured values should be less than the computed values, but only by  $1.7\% \pm 4\%$ . The source of the discrepancy of about 6% cannot be identified here; however, the modeled values do agree with observations from another satellite instrument (Multiangle Imaging Spectroradiometer), suggesting that the CERES calibration must be considered a possible source of the discrepancy.

**Citation:** Hudson, S. R., S. G. Warren, and S. Kato (2010), A comparison of shortwave reflectance over the East Antarctic Plateau observed by CERES to that estimated from surface reflectance observations, *J. Geophys. Res.*, 115, D20110, doi:10.1029/2010JD013912.

## 1. Introduction

[2] Uncertainties in angular distribution models (ADMs) used by the Clouds and the Earth’s Radiant Energy System (CERES) experiment for converting observed top-of-atmosphere (TOA) radiances to hemispheric fluxes over permanently snow-covered regions with clear skies were examined by Hudson *et al.* [2010]. This was done by comparing the angular distribution of reflected radiance from the ADMs with that from a radiative transfer model that used snow surface reflectance and atmospheric conditions based on measurements at Dome C station on the East Antarctic Plateau (75°S, 123°E, 3200 m). The details of the model are given in section 2 of the work of Hudson *et al.* [2010], and the terminology used to describe directional reflectance is explained in section 1 of the same work [Hudson *et al.*, 2010].

[3] In this paper we run the same model and compare the magnitude of reflected radiances and fluxes observed by CERES to those obtained from a model applied to surface observations, to compare the calibration of the CERES shortwave instruments and the model. The model was run as described by Hudson *et al.* [2010], but at 1° intervals of solar zenith angle ( $\theta_0$ ), with output saved at 2° intervals of viewing zenith angle ( $\theta_v$ ) and 3.75° intervals of relative azimuth ( $\phi$ ). The modeled radiance or flux at the solar zenith angle and viewing geometry of CERES observations is then determined by interpolating the stored values in solar zenith, viewing zenith, and relative azimuth angles.

[4] The broadband values from the model were calculated by integrating over wavelengths from 0.2 to 10  $\mu\text{m}$ , with thermal emission turned off. This full broadband range was chosen to allow a comparison with the most widely used CERES shortwave products, which are based on the “unfiltered” radiances. The unfiltering process, described by Loeb *et al.* [2001], converts the measured radiance, which is affected by instrument filtering and thermal emission, to an estimated total upwelling solar radiance integrated over all wavelengths. (The process might more accurately be called “defiltering.”) This is stated most clearly in the document describing the CERES SSF data product (<http://science>).

<sup>1</sup>Norwegian Polar Institute, Tromsø, Norway.

<sup>2</sup>Department of Atmospheric Sciences, University of Washington, Seattle, Washington, USA.

<sup>3</sup>Climate Science Branch, NASA Langley Research Center, Hampton, Virginia, USA.

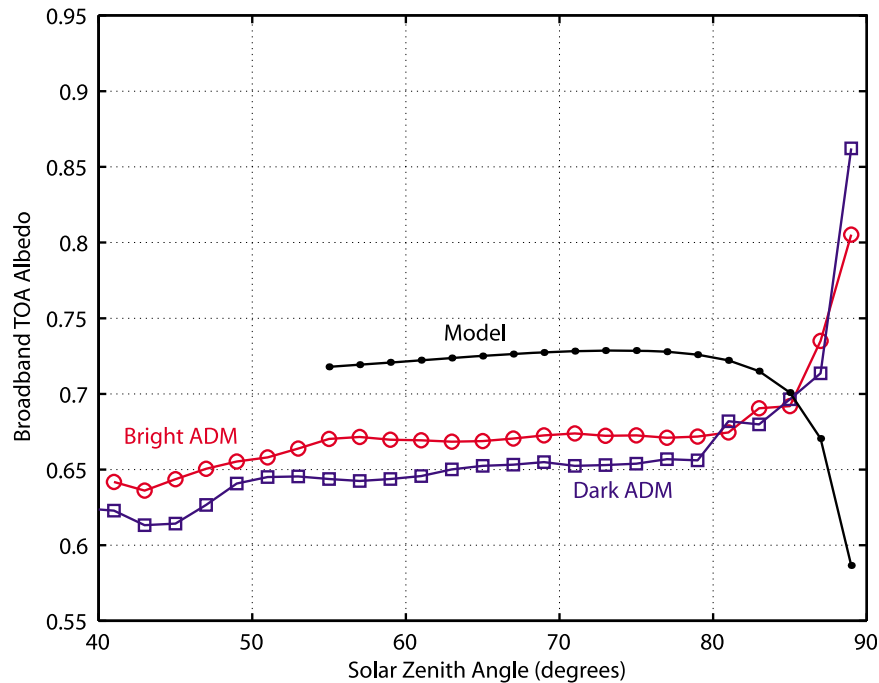


**Figure 1.** Comparison of broadband albedos, versus solar zenith angle, at the TOA from the CERES operational permanent-snow ADMs and from our model.

larc.nasa.gov/ceres/collect\_guide/pdf/SSF\_CG\_R2V1.pdf): The unfiltered shortwave radiance “is an estimate of the solar radiance at all wavelengths reflected back into space and contains no thermal radiance.... It is a spectrally integrated radiance that is intended to represent the radiance of reflected sunlight. In other words, the SW unfiltered radiance is the radiance we would observe if we had a spectrally flat channel that passed all the reflected sunlight and that removed any thermal emission from the Earth and the Earth’s atmosphere. Frequently, in informal discussion, we incorrectly refer to the SW unfiltered radiance as a broadband radiance covering the spectral interval from 0 to 5  $\mu\text{m}$ .”

[5] The Antarctic Plateau is a large, spatially and temporally homogeneous region of the planet, with a clean, dry, optically thin atmosphere, making it an appealing area for use in satellite-model comparisons. The region was previously used as a calibration target for an Advanced Very High Resolution Radiometer (AVHRR) [Loeb, 1997; Masonis and Warren, 2001].

[6] We begin by comparing the ADM albedos, which are representative of the mean albedo observed by CERES over all permanently snow-covered regions, to the model’s albedo. Following that, we examine the differences in more detail by comparing approximately 20,000 CERES radiances and fluxes observed on clear days in the region around Dome C with the modeled radiance and flux at the same solar and viewing angles. We then examine sources of uncertainty and try to explain the differences we find between the model and observations.

## 2. Comparison of Modeled and ADM Albedo

[7] Figure 1 compares the albedo from the CERES permanent snow ADMs [Kato and Loeb, 2005] with that from

the model. Kato and Loeb [2005] developed two clear-sky permanent-snow ADMs, differentiated by the surfaces’ nadir brightness; albedos from both ADMs are shown in Figure 1. The different shapes of the model and ADM curves at large solar zenith angles are due to the different geometry of the atmosphere and model. At these large solar zenith angles, a significant fraction of the reflected light at the TOA did not enter the atmosphere above the observation location but was scattered through the atmosphere to that location; the plane-parallel model used here does not account for this scattered light, which entered the atmosphere at a smaller zenith angle as a result of the Earth’s curvature. The model also overestimates the atmospheric path length compared to the real path length through the spherical atmosphere, therefore causing too much absorption of incident light at large solar zenith angles and absorption of upwelling light reflected by the surface into large viewing zenith angles. When the sun is high enough that the effect of Earth’s curvature is insignificant, there is a general trend of slightly increasing albedo as the solar zenith angle increases from 55° to 75°. This trend is caused by the increase in surface albedo with increase in solar zenith angle, especially at near-infrared wavelengths. Even in Antarctica, almost all of the solar energy received by the surface and atmosphere is at solar zenith angles of less than 80°, and at these angles the model albedos are higher than the ADM albedos by 0.05–0.08 (Figure 1). Investigation of that discrepancy is the aim of this paper.

[8] Dome C is one of the higher, drier permanent snow regions, with only 0.7 mm of precipitable water in the model summertime atmosphere used here. To see if this lack of water vapor could account for the albedo difference seen here, the model was run with a solar zenith angle of 75°, using the subarctic winter atmosphere [McClatchey et al.,

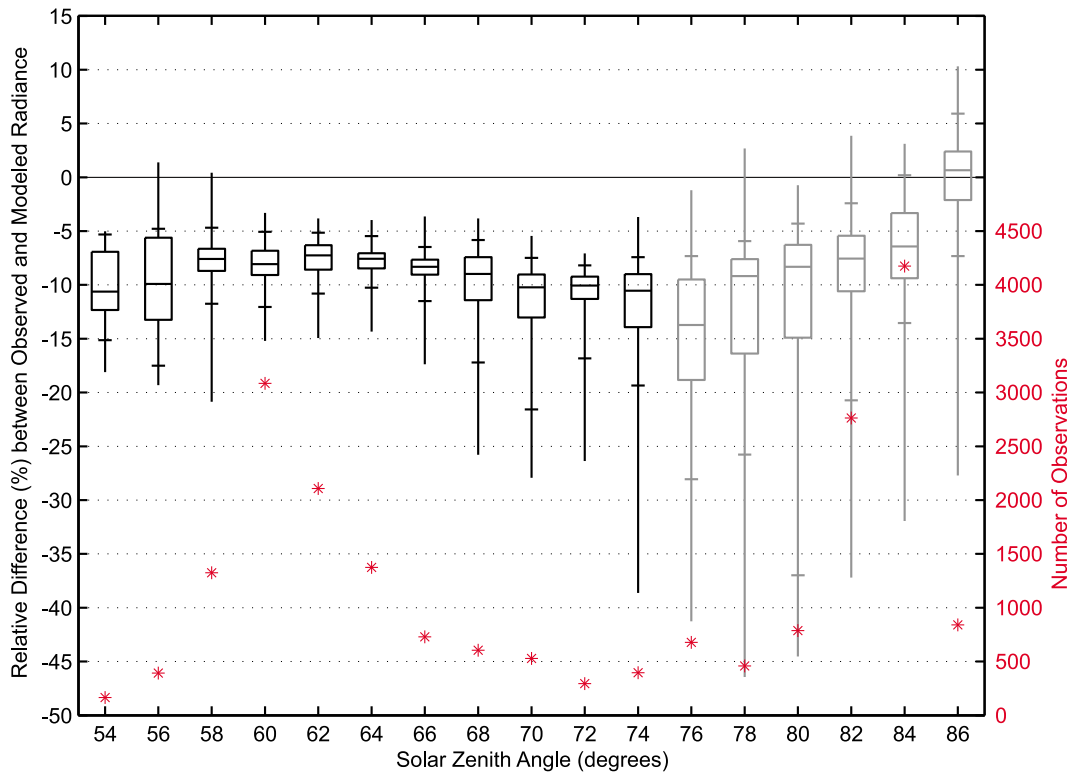


**Figure 2.** Boxplots showing the relative difference between the CERES-observed and the modeled radiances [ $100 \times (\text{CERES} - \text{Model})/\text{Model}$ ] within 200 km of Dome C as a function of solar zenith angle. Each boxplot shows the distribution of differences for all radiances used by CERES that were observed in the  $2^\circ$  range of solar zenith angles, regardless of viewing geometry; the boxes extend from the 25th to the 75th percentiles of the differences, with a horizontal line at the median; the vertical lines extend to the minimum and maximum differences, with horizontal ticks at the 5th and 95th percentiles. Values for observations made with  $\theta_0 > 75^\circ$ , where the model is less reliable, are plotted in gray. The number of observations used to create each boxplot is shown by the red asterisks, referring to the right-hand axis.

1972], which contains 4 mm of precipitable water. Using this atmosphere reduced the model albedo from 0.729 to 0.661, in line with the ADM albedos. Thus, the albedo difference could be explained if most of the permanent snow seen by CERES was under an atmosphere with large amounts of water vapor. However, varying the amount of water vapor is not likely to explain much of the difference, for the following reasons. First, most of Antarctica has less precipitable water than the subarctic winter atmosphere, even in the warmest month (January), according to the National Centers for Environmental Prediction/National Center for Atmospheric Research reanalysis. Second, the subarctic winter atmosphere has a column ozone amount of 486 Dobson units (DU), about 75% more than the January Antarctic atmosphere, according to NOAA Global Monitoring Division ozonesonde data and Global Ozone Monitoring Experiment data [Burrows *et al.*, 1999]. Third, Antarctica has eight times the area of Greenland, so most of the permanent snow scenes used by CERES to develop ADMs would have had water-vapor amounts far lower than Arctic values. Finally, a separate comparison was made with nonoperational CERES ADMs developed with data from

only the region around Dome C, and it showed similar differences between the model and ADM albedos.

### 3. Comparison With Individual Observations

[9] To try to assess the accuracy of the model output and of CERES radiance and flux data from observations over the area around Dome C, modeled radiances and fluxes are compared with CERES observations from this region. CERES observations from all four polar-orbiting instruments were used, and all were taken from Edition 2B-rev1 SSF data [Matthews *et al.*, 2005]. CERES data with surface footprints lying within 200 km of Dome C were gathered from 3 days in January 2004 and 1 day in January 2005, during times when our visual observations from the surface indicated that skies were free of clouds and boundary-layer ice crystals at Dome C Station for at least 6 h (data are from 9 overpasses on 13 January 2004 spread between 0600 and 2400 local standard time (UTC+8), 16 overpasses spread between 1700 on 18 January and 1800 on 19 January 2004, 8 overpasses spread between 1900 on 21 January and 0900 on 22 January 2004, and 3 overpasses around 0900, 1100,

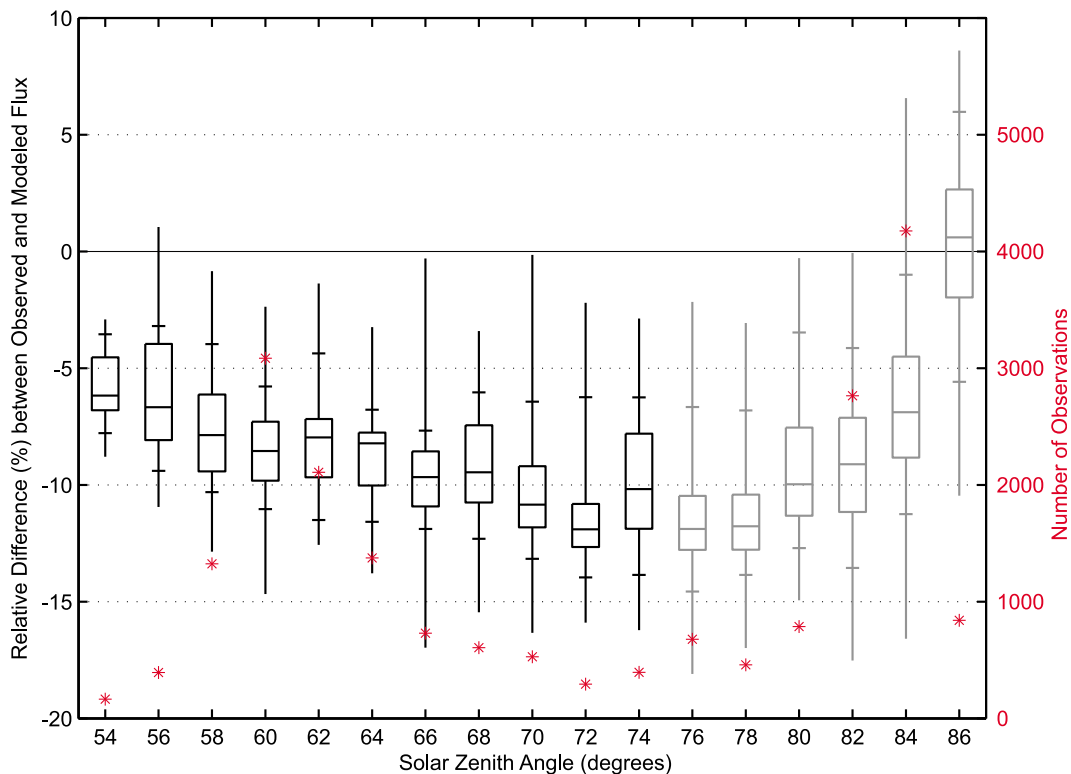


**Figure 3.** As in Figure 2, but for fluxes instead of radiances.

and 2200 on 28 January 2005). This provided 23,257 radiance observations that were used by CERES to determine fluxes (with  $\theta_0 < 86.5^\circ$  and  $\theta_v < 70.0^\circ$ ). Of these observations, 20,700 were identified by CERES as having clear skies, and only this subset was used in the comparison.

[10] The relative difference between each CERES radiance observation and the modeled radiance at the same solar zenith, viewing zenith, and relative azimuth angles was calculated along with the relative difference between each CERES flux calculation and the modeled flux at the same solar zenith angle. The results are summarized, as functions of solar zenith angle, in Figures 2 and 3. In each of these figures, the data are grouped into  $2^\circ$  bins in  $\theta_0$  and are summarized with boxplots that show, for each bin, the median difference, the upper and lower quartiles, the 5th and 95th percentiles, and the range of differences. The figures also show the number of observations in each bin, which varies significantly because the satellites' orbits cause them to pass near Dome C most often in midmorning and late evening, local time. The figures for both radiance and flux differences are included because, although the radiance data are closer to the actual observations made by the CERES instruments, the flux data are more widely used.

[11] The general pattern seen in these figures is that the CERES radiances and fluxes are smaller than the modeled values, with a median difference of about 8%. As discussed in section 2, the plane-parallel model results in errors in the modeled reflectance that become increasingly significant at  $\theta_0$  larger than  $75^\circ$ – $80^\circ$ . This error results in too little reflectance from the model at large solar zenith angles, which shows up in the figures as a better agreement between the

observations and model at the largest solar zenith angles. Because this is caused by a deficiency in the model, we include in the remainder of the discussion only the 11,000 observations we have that were made with  $\theta_0 < 75^\circ$ . Comparing Figures 2 and 3, we see that the outlying data with large negative differences in the radiance plot have the magnitude of their differences significantly reduced in the flux plot. This is because of differences between the model and CERES anisotropic reflectance patterns [see Hudson *et al.*, 2010], which can cause the relative difference in the flux estimate to differ from the relative difference in the radiance measurement.

[12] Those large differences represent a small fraction of the data; fewer than 3% of the radiance observations differ from the model by more than 15%, whereas 77% of the observations differ from the model by between  $-5\%$  and  $-10\%$ , with a median of  $-8.1\%$ . The median difference between CERES and modeled fluxes is  $-8.4\%$ . Taking observations from the four polar-orbiting CERES instruments separately (there are two CERES instruments on the Terra satellite, called FM1 and FM2, and two on the Aqua satellite, called FM3 and FM4), the median radiance differences are  $-7.3\%$  for FM1,  $-7.1\%$  for FM2,  $-9.0\%$  for FM3, and  $-9.0\%$  for FM4. The median flux differences for the four instruments are  $-7.4\%$ ,  $-7.6\%$ ,  $-10.0\%$ , and  $-10.3\%$ . Examining the differences as a function of viewing zenith angle of the observations (from  $0^\circ \leq \theta_v < 70^\circ$ ) showed no variation in the median difference, but it did show an increase in the range (and to a lesser extent, the interquartile range) of the differences within each  $\theta_v$  bin, with increasing  $\theta_v$ .

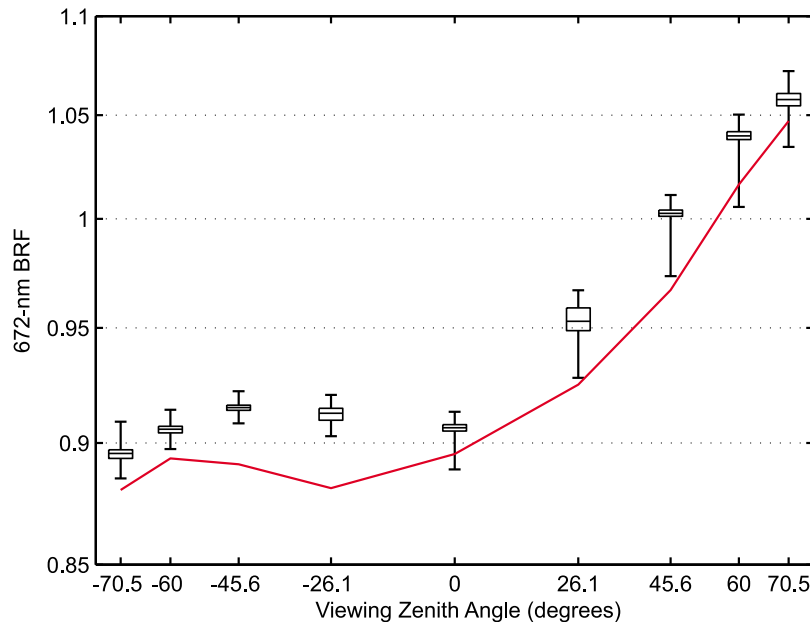


**Figure 4.** Boxplots showing MISR red-channel BRF observations from within 50 km of Dome C during one overpass, at 0820 local standard time 28 December 2003 (0020 UTC, 28 December 2003); they show the median, upper and lower quartiles, and the range. The modeled BRF for the same solar zenith angle ( $58^\circ$ ) and relative azimuth angles (approximately  $30^\circ$  for  $\theta_v > 0$ ,  $150^\circ$  for  $\theta_v < 0$ ) is shown in red.

[13] Some scatter is to be expected in comparisons between CERES observations and the model because the model has an atmosphere and snow surface that are representative of average summer conditions at Dome C, but the CERES observations see both spatial and temporal variability. However, the consistent bias seen in Figures 2 and 3 suggests that the model overestimates the reflectance, CERES underestimates the reflectance, or both. To try to see if we should conclude that the model is overestimating the reflectance, modeled reflected radiances at four wavelengths were compared with the radiances observed within 50 km of Dome C by the Multiangle Imaging Spectroradiometer (MISR [Diner *et al.*, 1998]) during four overpasses of Dome C, with clear sky and solar zenith angles between  $57^\circ$  and  $64^\circ$ . MISR observes the light reflected from a location at nine viewing angles within 10 min, allowing comparisons to be made over a variety of viewing angles. Its four spectral channels lie in the blue, green, red, and near-infrared regions.

[14] A representative example of these comparisons, using the 672 nm (red) channel, is shown in Figure 4. This figure shows the distribution of observed bidirectional reflectance factors (BRFs, equal to  $\pi$  times the reflected radiance, divided by the incident flux) and the corresponding modeled BRF. In these comparisons, the shape of the modeled reflectance versus viewing zenith angle compares well with the MISR observations. Of the 144 individual comparisons made (four overpasses with nine cameras, each with four channels), the modeled reflectance was above the MISR-observed range of reflectance only 5 times; it was in the upper quartile of the range 8 times, within the interquartile range 22 times, in the lower quartile 29 times, and below the range of observed values 80 times. The median radiance difference [(MISR - Model)/Model] of all observations

within 50 km of Dome C from the four overpasses is +3.0%, and the interquartile range is +0.9% to +4.7%. Thus, whereas the model broadband radiance exceeds the CERES broadband radiance, the model spectral radiance is usually lower than the MISR spectral radiance.

[15] The absolute uncertainty in MISR radiances is estimated to be within 4% (one standard deviation level of confidence) for bright, uniform targets [Bruegge *et al.*, 2002; MISR data quality statement available at [http://eosweb.larc.nasa.gov/PRODOCS/misr/Quality\\_Summaries/L1\\_Products\\_20040310.html](http://eosweb.larc.nasa.gov/PRODOCS/misr/Quality_Summaries/L1_Products_20040310.html)]. That large uncertainty means that this comparison cannot be taken as proof that CERES is under-reporting the reflected radiance near Dome C. We must now examine known uncertainties in the model and in the CERES observations to see what can be said about the differences between the CERES-observed and modeled radiances.

#### 4. Uncertainties

[16] In this section we examine uncertainties in both the model and the observations to try to determine if the differences presented in section 3 are statistically significant. Potential sources of error in the modeled reflectance fall into four main categories: (1) the albedo specified at the lower surface may be biased or affected by random variability; (2) the parameterization of the anisotropic reflectance factor used for the lower boundary in the model may be in error; (3) the atmospheric model may incorrectly handle gaseous absorption, or atmospheric variability may affect the results; and (4) the solar spectrum used in the model may differ from what was incident at the time of the observations. In sections 4.1–4.6, we consider each of these sources in detail and then estimate the 95% confidence interval around

the expected difference between the CERES-observed and modeled radiances and fluxes.

#### 4.1. Albedo

##### 4.1.1. Error in the Albedo Measured at Dome C

[17] The snow-surface albedo measured under a cloud at Dome C and presented by *Hudson et al.* [2006] is used in the parameterization of the anisotropic reflectance factor ( $R$ ) and was also used to determine the best snow grain sizes to use for modeling the spectral albedo as a function of solar zenith angle (see section 2 of the work by *Hudson et al.* [2010] and section 4 of the work by *Hudson and Warren* [2007]). There is naturally some uncertainty in this measurement; however, this uncertainty does not directly affect the model results presented in sections 2 and 3 but rather affects the uncertainty of the modeled surface albedo and of the parameterization of  $R$ , both of which are discussed below. For this reason, we only briefly discuss these uncertainties, and they are not included in Table 1, which lists the uncertainties affecting the measurements and model.

[18] The largest source of uncertainty in the albedo measurement is the correction that had to be applied to the raw measurements to account for the shadow of the instrument and observer. Two separate methods were used to determine this correction, one geometrical and the other based on consistency in derived grain sizes at different wavelengths; both suggested the raw albedo must be increased by about 4% to obtain the actual albedo. We applied the correction from the geometrical method, increasing the measured albedo by 4.2% to obtain the actual albedo. We estimate that the uncertainty of the albedo, due to this correction, is about  $\pm 1\%$ .

[19] The albedo measurement consists of a ratio of two flux spectra, both made with the same instrument and cosine collector, so the calibration of the instrument does not affect the resulting albedo. On the evening when the albedo was measured, there was a thick overcast that diffused the solar beam, minimizing errors due to imperfect cosine response and errors due to tilt of the instrument or surface. The measured albedo was determined by averaging 10 albedo observations made over a period of about 10 min. The standard deviation of the 10 broadband (350–2400 nm) albedos is 0.0036 (0.46%). This provides a good estimate of the uncertainty in the measurement that is not related to the shadowing correction.

[20] The snow surface above which the albedo at Dome C was measured was smoother than most of the snow around Dome C. Wind-erosion features called sastrugi are responsible for the surface roughness on the Antarctic Plateau. The Dome C region has smaller sastrugi than most of Antarctica because of the light winds that are found there, but accurately measuring the albedo above even small sastrugi would require being well above the surface. Therefore, an unrepresentatively smooth region of snow was chosen for the measurement. Taking 0.1 as the typical height-to-width ratio of sastrugi at Dome C (see section 3.1 of the work of *Hudson et al.* [2006] for a description of the snow surface roughness at Dome C), along with results from the work of *Warren et al.* [1998, Figure 13b] and with the spectral albedo from Dome C, we estimate that the broadband albedo over the smooth snow may be up to 0.0065 (0.8%) too high compared to that for the rough surface.

##### 4.1.2. Error in the Modeled Surface Albedo

[21] The modeled albedo is used in two ways in this paper: first, the modeled diffuse albedo is used to provide the necessary input to the parameterization of  $R$  at wavelengths longer than  $2.4 \mu\text{m}$ , for which we did not measure the albedo; second, the modeled direct-beam albedo for all incidence angles is used to convert  $R$ , a normalized directional reflectance, to the BRF.

[22] The modeled diffuse albedo is used only for the calculation of  $R$  at wavelengths longer than  $2.4 \mu\text{m}$ . Errors in this modeled albedo would lead to an incorrect angular distribution of reflected flux at those long wavelengths but would not affect the amount of reflected flux at the surface. Because only about 0.1% of the reflected flux is at wavelengths longer than  $2.4 \mu\text{m}$  under a clear sky with  $\theta_0 = 60^\circ$ , errors in the modeled diffuse albedo do not have any significant impact on our results.

[23] The modeled direct-beam albedo is more important; it is used to convert the calculated  $R$  to a BRF and therefore determines the overall albedo of the surface. This albedo had to be modeled because accurately observing the direct-beam spectral albedo under all incidence angles was not possible on the natural snow. (The albedo at all incident zenith angles, even those never obtained by the sun, must be known so that the model can handle diffuse incidence, and the albedo must be for pure direct-beam incidence, not the natural mix of direct and diffuse found at the surface.)

[24] We modeled the albedo in SBDART with no atmosphere and with two snow layers: a semi-infinite layer of  $90 \mu\text{m}$  grains below a  $0.25 \text{ mm}$  layer of  $40 \mu\text{m}$  radius grains. The snow grains were specified as having the single-scattering albedo of an ice sphere of the given radius and a Henyey-Greenstein phase function with asymmetry factor of an ice sphere of the given radius. The Mie calculations were performed using the updated ice absorption coefficients from the work of *Warren et al.* [2006]. *Grenfell et al.* [1994] found that such a two-layer snow model was better able to match Antarctic albedo measurements because the natural snow often has small grains at the very surface because they are the last to fall back to the surface after blowing snow events. The two grain sizes were determined by modeling the albedo under a thick cloud with the specified grain sizes of the two layers varying from 20 to  $120 \mu\text{m}$ , and finding which combination best matched the observed albedo under a cloud [by minimizing the root-mean-square error (RMSE) over all wavelengths].

[25] Errors in the specified grain sizes and in the single-scattering properties of the grains, as well as uncertainty in the ice absorption spectrum, all combine to create uncertainty in modeled albedo. Using a different model and different methods, Richard Brandt and Stephen Warren (personal communication, 2009) used the same albedo measurement and estimated the snow to have  $50 \mu\text{m}$  grains over  $80 \mu\text{m}$  grains. Comparing modeled clear-sky albedo with  $\theta_0 = 60^\circ$  for snow grains of 30 to  $50 \mu\text{m}$  over snow grains of 80 to  $100 \mu\text{m}$  indicates an uncertainty in the modeled albedo due to grain size uncertainty (full range of these modeled albedos) of 0 to  $\pm 0.0023$  in the visible (increasing with wavelength), increasing to  $\pm 0.029$  at  $1.3 \mu\text{m}$  and to  $\pm 0.045$  at  $2.25 \mu\text{m}$ . The resulting uncertainty in the broadband albedo is  $\pm 0.009$ , which is  $\pm 1.1\%$ . Because we

looked at the full range of the different albedos, we take this to be a  $2\sigma$  uncertainty due to grain size uncertainty.

[26] The Henyey–Greenstein phase function was used for modeling the spectral albedo. This represents a computational convenience, not an attempt to accurately describe the real phase function. Nevertheless, it is often used in atmospheric radiative transfer modeling and was shown by *Hansen* [1969] to result in accurate albedo calculations for conservatively scattering, optically thick clouds. More recently, *Aoki et al.* [2000] showed that it can be used to accurately model reflectance from snow, with differences between the spectral albedo modeled with the full Mie phase function and that modeled with the Henyey–Greenstein phase function of around 0.0015 or less at all wavelengths from 0.35 to 2.5  $\mu\text{m}$  (their Figure 14). If we take an uncertainty in the modeled spectral albedo due to the choice of phase function of  $\pm 0.0015$ , it gives an uncertainty in the broadband albedo under clear sky with  $\theta_0 = 60^\circ$  of  $\pm 0.2\%$ .

[27] There remains some uncertainty regarding the complex index of refraction of pure ice, which is used as an input to the Mie calculations that determine the single-scattering properties of the snow grains. *Warren and Brandt* [2008] recently published an updated compilation of the complex index of refraction of ice. For our model, the most important difference between the new values and the old standard [*Warren*, 1984] is reduced absorption in the ultraviolet and shortwave visible wavelengths, based on the results of *Warren et al.* [2006]. To estimate the uncertainty in the modeled albedo due to uncertainty in the ice optical properties, we compare the albedo modeled with the newly compiled values to those modeled with the older compilation. Under clear sky with  $\theta_0 = 60^\circ$ , spectral albedo differs by up to 0.04; the broadband albedo is 0.3% higher with the newly compiled values. On the basis of this result, we take an uncertainty in modeled albedo of  $\pm 0.3\%$ .

[28] Combining the three sources of uncertainty gives an overall uncertainty in the modeled radiance and flux due to uncertainty in the calculated albedo of  $\pm\sqrt{1.1^2 + 0.2^2 + 0.3^2} = \pm 1.2\%$ . We consider this to be a good estimate of the  $2\sigma$  uncertainty of the broadband albedo at the surface under the clear, Dome C model atmosphere. This error is taken to be a bias of unknown sign, because increasing the number of observations used in the comparison does not reduce the effect of this uncertainty. We can also include the bias due to sastrugi, as discussed in section 4.1.1, in which the albedo of the modeled flat surface is potentially up to 0.8% higher than that of the natural snow surface.

#### 4.1.3. Spatial and Temporal Variability of Albedo

[29] Previous studies of broadband albedo on the East Antarctic Plateau have shown values in December and January varying between about 0.8 and 0.87, without much variability among South Pole, Dome C, Vostok, and Plateau stations [*Grenfell et al.*, 1994; *Pirazzini*, 2004; *Kuhn et al.*, 1977]. The lack of any systematic variability in the albedo at the different stations indicates that we need to concern ourselves mostly with temporal variability. Most of the variability that is reported is due to variability of solar zenith angle and cloudiness. Our modeled spectral albedos result in broadband albedos that vary from 0.809 at  $\theta_0 = 50^\circ$  to 0.887 at  $\theta_0 = 89^\circ$ .

[30] From the data presented for December 1966 and January 1967 in Figure 7 of the work by *Kuhn et al.* [1977],

we calculated a standard deviation of daily mean summertime albedo at the Plateau station of 0.018, which is 2.2% of the mean of the daily albedos (0.825). Data obtained from the NOAA observatory at the South Pole for January 2007, 2008, and 2009 showed a clearly increasing albedo from year to year (the January mean albedo was 0.851, 0.874, and 0.899 in 2007, 2008, and 2009), which is almost certainly a spurious trend. Therefore, the standard deviation of the departure of the daily mean albedo from the monthly mean albedo for that particular January was calculated for this 3 month data set, and also happened to be 0.018. Some of the variability at both stations is due to day-to-day changes in cloudiness and solar zenith angle, so we assume that a little more than half of the variability is due to real temporal changes in the snow, and we estimate that the  $2\sigma$  uncertainty in an individual comparison between our model results and a CERES observation, due to spatial and temporal albedo variability, is around  $\pm 2.5\%$ . Assuming we can consider the 4 days from which observations were used in the comparisons as independent samples, then this uncertainty is reduced to  $\pm 2.5\%/\sqrt{4} = \pm 1.25\%$  for the overall comparison.

#### 4.2. Anisotropic Reflectance Factor

[31] Sections 4.1.1–4.1.3 discuss the uncertainty in the model's specification of the reflected surface flux, but the modeled radiances are also affected by the uncertainty in the model's specification of the angular distribution of this reflected flux. This distribution is taken from the parameterization for the surface anisotropic reflectance factor presented by *Hudson et al.* [2006]. Table 1 of the work of *Hudson et al.* [2006] gives the RMSE of the parameterized values of  $R$  for different ranges of  $\lambda$ ,  $\theta_0$ , and  $\theta_v$ . Ignoring the contribution of error in individual measurements to the RMSE, we take these values to be representative of the  $1\sigma$  uncertainty due to the parameterization.

[32] Around 80% of the reflected energy at the TOA is at  $\lambda < 950$  nm, and most of the viewing zenith angles in the CERES-model comparisons were  $52.5^\circ$  or less, so we use the RMSE for the parameterization for  $350 \leq \lambda \leq 950$  nm, calculated for  $\theta_v \leq 52.5^\circ$ , which is 1.9% for  $\theta_0 < 75^\circ$  and 3.0% for  $\theta_0 > 70^\circ$ . Averaging these two values, we estimate the  $1\sigma$  uncertainty due to the parameterization is  $\pm 2.5\%$ . Much of this uncertainty represents variability in  $R$ , but some is also due to errors in the parameterization. Because we cannot accurately separate the two contributions, we assume only two, rather than four, independent samples, reducing the  $2\sigma$  uncertainty estimate from  $\pm 5\%$  to  $\pm 3.5\%$ .

[33] As described by *Hudson et al.* [2010], the surface  $R$  at all wavelengths less than 800 nm was assumed to be equal to that at  $\lambda = 800$  nm. This was done because the measurements, and therefore the parameterizations, of  $R$  at shorter wavelengths are affected by diffuse incidence from Rayleigh scattering, and because the direct-beam  $R$  correlates well with albedo, which does not change much between 800 and 300 nm. The accuracy of this assumption was tested in section 5.3 of the work by *Hudson et al.* [2006], where their Figure 15 shows the relative error caused by assuming  $R$  at 375 nm was equal to  $R$  at 900 nm. This shows that, for most  $\theta_v < 70^\circ$ , the error is within  $\pm 3\%$ . This represented an extreme test for this assumption (starting with 900 nm, rather than 800 nm, and comparing with the wavelength with the highest albedo), and only 65%–

70% of the reflected energy is affected by this assumption, so we estimate the  $2\sigma$  uncertainty associated with this assumption to be  $\pm 2.5\%$ .

[34] Combining these two uncertainties related to the parameterization of  $R$  gives an overall uncertainty for an individual radiance comparison of  $\pm\sqrt{3.5^2 + 2.5^2} = \pm 4.3\%$ . The sign and magnitude of the error in the parameterized  $R$  varies with viewing and solar geometry. Therefore, when we combine all of our comparisons from different solar and viewing angles, the effect of this uncertainty is reduced. We used observations made with various combinations of  $\theta_v$  from  $0^\circ$  to  $70^\circ$ ,  $\theta_0$  from  $54^\circ$  to  $75^\circ$ , and all relative azimuth angles; we assume that this gives us at least 10 independent samples in the  $\theta_v$ - $\phi$ - $\theta_0$  space, reducing this uncertainty to  $\pm 4.3/\sqrt{10} = \pm 1.4\%$ . This uncertainty affects only the radiance comparisons, not the flux comparisons.

### 4.3. Atmospheric Model

#### 4.3.1. Error in Modeled Gaseous Absorption

[35] Here we attempt to assess the uncertainty in the model results due to errors in the specification of gaseous absorption in the radiative transfer model. The model we used, Santa Barbara DISORT Atmospheric Radiative Transfer Model (SBDART), was one of the models entered into an inter-comparison study presented by *Halothore et al.* [2005], which examined the performance of 16 shortwave radiative transfer models in various case studies, including one with a clear, aerosol-free, subarctic winter atmosphere and a solar zenith angle of  $75^\circ$ . From the results of *Halothore et al.* [2005], we see that SBDART and the related model Santa Barbara Moderate Resolution Radiative Transfer Algorithm (SBMOD; which uses the HITRAN, rather than LOWTRAN-7, absorption data) both calculated more atmospheric absorption than most of the other models (SBDART calculated that the atmosphere absorbs 19.9% of the flux incident at the TOA, while the mean and standard deviation from all 15 models were 18.9% and 0.9%). This increased absorption resulted from higher near-infrared absorption in SBDART than in the other models.

[36] If the model produces too much atmospheric absorption at wavelengths where the surface albedo is low, it will have less of an effect on the TOA reflectance than if it does so where the albedo is high, because much of the extra energy absorbed by the atmosphere would have been absorbed by the surface anyway. In the near-infrared band used by *Halothore et al.* [2005] ( $0.7$ – $5.0 \mu\text{m}$ ), about half of the atmospheric absorption in our model occurs at wavelengths where the snow albedo is less than 0.5. This distribution of the atmospheric absorption will reduce the overall effect on the TOA reflectance results, compared to what it would be if the (presumably spurious) absorption occurred at visible wavelengths, where the snow is very bright. Further minimizing the importance of this potential model error is the fact that our Dome C model atmosphere has about one sixth as much water vapor as the subarctic winter atmosphere, leading to a reduction in the atmospheric absorption in this near-infrared band of about 45%.

[37] *Halothore et al.* [2005] reported a standard deviation of broadband atmospheric absorptance, among the models they tested, of 4.7% of the mean absorptance in all models. With a solar zenith angle of  $70^\circ$ , 4.7% of the atmospheric

absorptance in our model is  $3 \text{ W m}^{-2}$ , or 0.87% of the TOA reflected flux. We reduce this uncertainty by 25% to account for the fact that surface absorption partially compensates for errors in atmospheric absorption, and then we double it to get a  $2\sigma$  uncertainty of  $\pm 1.3\%$  due to uncertainty in gaseous absorption in the model. We could choose to use the results of *Halothore et al.* [2005] to specify a negative bias in the modeled reflected flux, but because it is not clear which, if any, of the tested models is right, we choose to define this as an uncertainty of unknown sign.

#### 4.3.2. Spatial and Temporal Variability of the Atmosphere

[38] The model was run with an atmosphere that is representative of the mean atmospheric conditions over Dome C in summer. Here we attempt to assess the uncertainty due to atmospheric variability. All of the CERES observations considered were made within 200 km of Dome C, where the surface elevation does not change much, so we do not need to consider the full range of atmospheric variability over permanent snow as we did in a previous study [*Hudson et al.*, 2010]. Instead, we ran the model in four modified configurations: (1) with twice as much precipitable water, (2) with half as much precipitable water, (3) with an increase in total ozone concentration of 20 DU, and (4) with a decrease in total ozone concentration of 20 DU. Other than the stated changes, the model was configured exactly as in the standard runs, with a solar zenith angle of  $70^\circ$ . The choice of ozone variability was made based on daily observations of ozone concentration over Dome C made in January 2004 and 2005 by the Total Ozone Mapping Spectrometer, which showed a mean value of 281 DU and a standard deviation of 9 DU.

[39] Halving or doubling the precipitable water caused an increase of 1.1% or a decrease of 1.4% in the TOA reflected flux, and it changed the TOA reflected radiances at the viewing angles used by CERES by up to  $\pm 1.8\%$ . Changing the total column ozone amount by  $\pm 20$  DU changed the TOA reflected flux by  $\pm 0.3\%$ , and it changed the TOA reflected radiances at the CERES viewing zenith angles by up to  $\pm 0.35\%$ . On the basis of these results, we take the uncertainty in individual comparisons due to atmospheric variability to be  $\pm\sqrt{1.8^2 + 0.4^2} = \pm 1.8\%$ . Again assuming four independent samples, this is reduced to  $\pm 0.9\%$ .

### 4.4. Solar Spectrum

#### 4.4.1. Incident Broadband Flux

[40] The LOWTRAN-7 solar spectrum was used in our model, adjusted for the Earth-Sun distance on the day each observation was made. This spectrum provides an incident flux at the top of the atmosphere of  $1372.3 \text{ W m}^{-2}$  with an Earth-Sun distance of 1 AU. Newer estimates of the solar constant are closer to  $1366 \text{ W m}^{-2}$  with temporal variability on the order of  $\pm 0.15\%$  [*Fröhlich*, 2006], and some estimates from the Solar Radiation and Climate Experiment (SORCE [*Rottman*, 2005]) set the solar constant as low as  $1360 \text{ W m}^{-2}$  [*Lean et al.*, 2005; *Woods et al.*, 2009].

[41] If the lowest values are accurate, the TOA incident flux in the model was 0.9% higher than it was in reality. This means our modeled reflected fluxes and radiances have a positive bias of about  $0.9\% \pm 0.15\%$ . This bias affects only the direct comparisons of radiance or flux, as shown in

**Table 1.** A Summary of the Uncertainties Involved in the Comparison Between the CERES Observations and Our Model<sup>a</sup>

Source	Radiance		Flux	
	Known Sign	Unknown Sign	Known Sign	Unknown Sign
Modeled surface albedo	-0.8	±1.2	-0.8	±1.2
Albedo variability		±1.3		±1.3
$R$ parameterization		±1.4		
Gaseous absorption		±1.3		±1.3
Atmospheric variability		±0.9		±0.9
Incident TOA broadband flux	-0.9	±0.2	-0.9	±0.2
Solar spectral distribution		±1.0		±1.0
CERES data and processing		±2.2		±2.5
Total	-1.7	±3.7	-1.7	±3.6

<sup>a</sup>Some uncertainties or errors have a known sign, but the rest are biases or random uncertainties of unknown sign, given here as our best estimate of their  $2\sigma$  values, with a total calculated as the root-sum-square of the individual values. The uncertainties for radiance and flux comparisons are listed separately because some apply to only one or the other. All numbers are in %, and when signed, a positive number indicates something that leads to  $(\text{CERES} - \text{Model})/\text{Model} > 0$ .

Figures 2 and 3, not comparisons of quantities that are normalized by the incident flux, such as albedo or BRF.

#### 4.4.2. Spectral Distribution of Solar Flux

[42] In addition to the total solar flux incident at the top of the atmosphere, the spectral distribution of the incident energy is also important for determining the reflected radiance and flux. We ran the model using a solar spectrum measured on 15 January 2005 by SORCE. The SORCE spectrum extends only to  $\lambda = 2.4 \mu\text{m}$ ; beyond this, the spectrum was assumed to be that of a blackbody with a temperature equal to the blackbody temperature determined from the SORCE flux at  $\lambda = 2.4 \mu\text{m}$ . At wavelengths between 0.4 and  $2 \mu\text{m}$ , the SORCE and LOWTRAN spectral fluxes differ by up to  $\pm 10\%$ , whereas at shorter wavelengths the differences are up to  $\pm 45\%$ . At longer wavelengths the SORCE fluxes are about  $10\% \pm 10\%$  larger than the LOWTRAN fluxes. The main effect of the switch in incident spectra is to reduce the incident flux at  $\lambda < 0.9 \mu\text{m}$  and to increase it between 1.5 and  $4 \mu\text{m}$ .

[43] The shift of energy to longer wavelengths resulted in a reduction of TOA albedo with  $\theta_0 = 60^\circ$  of 0.0052, or 0.72%. After adjusting for the small difference in broadband flux between the two incident spectra, the reflected TOA radiances were reduced by 0.54 to 0.77%. On the basis of this test, we estimate that the uncertainty in the model results from uncertainty in the spectral distribution of solar energy is about  $\pm 1\%$ .

#### 4.5. CERES Instrument and Processing

[44] Dong *et al.* [2008] estimated the  $2\sigma$  uncertainty in CERES-observed shortwave broadband radiance to be  $\pm 2\%$ , with negligible random noise. An additional source of uncertainty in the CERES measurements comes from the “unfiltering” process, in which a model-derived regression analysis is used to estimate the total amount of reflected solar radiance, at all wavelengths, from the observed upwelling radiance in the CERES shortwave channel. This unfiltering process makes use of the CERES observations from the shortwave- and longwave-window channels, and it removes the spectral filtering of the instrument (i.e., accounts for the spectral response function) and eliminates the component of the upwelling radiance that is observed by the instrument that is from thermal emission. Loeb *et al.* [2001] developed the unfiltering method and estimated the  $2\sigma$  uncertainty associ-

ated with it to be  $\pm 0.8\%$ . Therefore, the overall uncertainty in the CERES radiance observations is  $\pm 2.2\%$ .

[45] A third source of uncertainty must be considered for the CERES fluxes: that associated with the radiance-to-flux conversion using the CERES angular distribution models. On the basis of the results presented by Hudson *et al.* [2010], we estimate this to be  $\pm 4\%$  for individual flux comparisons. As in section 4.2, this error varies with viewing and solar geometry. If we again assume 10 independent samples in this geometric space, then this uncertainty in the overall flux comparison is reduced to  $\pm 1.3\%$ , giving a total uncertainty in the CERES fluxes for the overall comparison of  $\pm 2.5\%$ .

#### 4.6. Summary of Uncertainties

[46] The uncertainties discussed throughout this section are summarized in Table 1. When combined, they indicate that we should expect, with 95% confidence, that the relative difference between the CERES observations and the modeled reflectance  $[(\text{CERES} - \text{model})/\text{model}]$  should be  $-1.7\% \pm 3.7\%$  for radiances and  $-1.7\% \pm 3.6\%$  for fluxes. However, the mean difference in our comparison of measured and modeled radiances is  $-8.5\%$  (median is  $-8.1\%$ ), and the mean difference in our flux comparison is  $-8.6\%$  (median is  $-8.4\%$ ), both of which are well outside our expected range. (These numbers were calculated from only those comparisons with  $\theta_0 < 75^\circ$  because of deficiencies in the plane-parallel model at larger angles; including those comparisons at larger  $\theta_0$  does not change the conclusion.) This result differs from that presented by Dong *et al.* [2008], who found that modeled and observed TOA albedos of deep convective clouds differ by  $-1\%$  (0.007 of the average albedo of 0.71), with a 95% confidence interval of  $\pm 5\%$ .

[47] In this section we tried to thoroughly evaluate the known potential errors associated with the modeling, and they are unable to explain the differences we found between the observations and the model. This suggests that either the CERES shortwave instruments have a negative calibration bias (at least over the Antarctic Plateau, which is unusually highly reflective at short solar wavelengths) or our model is missing a source of absorption in the Antarctic atmosphere-snow system. We cannot say conclusively from this study which, or what combination of these, is the answer, but given that CERES is our best monitoring system of Earth’s radiation budget, and that SBDART seems to compare

reasonably well with today's other atmospheric radiative transfer models, it is an important discrepancy.

## 5. Summary

[48] The broadband albedo of the Antarctic snow surface has been measured over many years by various research groups at different locations, and values have been obtained between 0.80 and 0.87. It was therefore a surprise when CERES obtained albedos of 0.67 at TOA, because it seemed unlikely that atmospheric absorption in the thin, dry atmosphere could be large enough to explain the difference. That puzzle was the motivation for undertaking the study reported in this paper.

[49] By using a parameterization of the surface reflectance of the East Antarctic Plateau, based on a set of detailed measurements made there, as the lower boundary in an atmospheric radiative transfer model, we eliminated what we believe to be the largest source of uncertainty in modeling solar radiative transfer over the region: modeling the snow-surface reflectance. The modeled reflectance at the TOA is around 7% less than the CERES observations, after accounting for known biases in the model. A detailed uncertainty analysis suggests (with over 99% confidence) that the two values should be within 5.6% of each other, indicating there is a source of uncertainty that has not been properly accounted for.

[50] We cannot say with certainty whether the unexpected difference between the observations and the model are a result of modeling error, observation error, or a combination of the two. Regardless, it is a discrepancy that must be investigated further because both CERES and SBDART (and models similar to it) are widely used. The modeled reflectances show better agreement with another satellite instrument (MISR), with a mean difference of the opposite sign. Because of uncertainties in the MISR data, we cannot be certain that the source of the CERES-model discrepancy lies in the CERES calibration; however, the MISR comparison does suggest that this possibility should not be ignored. Furthermore, the discrepancy was about 2% larger for observations from the Aqua satellite than for those from Terra, suggesting a possible difference between different CERES instruments.

[51] The East Antarctic Plateau was a useful place to perform this comparison because the clean, thin, dry atmosphere makes atmospheric modeling less uncertain, and the spatially and temporally homogeneous surface reduces the problems associated with temporal variability and with spatial matching of the satellite observations and ground comparison point. However, it is an extreme case in terms of the total flux and the spectral distribution of flux leaving the top of the atmosphere. It is therefore possible that the unidentified source of uncertainty has a smaller effect over other darker, or spectrally different, regions.

[52] **Acknowledgments.** We thank Richard Brandt, Bruce Wielicki, Norman Loeb, Tom Charlock, and Zhonghai Jin for useful discussions, and two anonymous reviewers who provided comments that improved the paper. David Longenecker provided the NOAA ESRL radiation data from the South Pole that were used in section 4.1.3. CERES and MISR data were obtained from the Atmospheric Science Data Center at the NASA Langley Research Center. This research was supported by National Science Foundation grants OPP-00-03826 and ANT-06-36993. Hudson also received funding from the Norwegian Research Council through its IPY programme and the project iAOS Norway (grant 176096/S30).

## References

- Aoki, T., T. Aoki, M. Fukabori, A. Hachikubo, Y. Tachibana, and F. Nishio (2000), Effects of snow physical parameters on spectral albedo and bidirectional reflectance of snow surface, *J. Geophys. Res.*, *105*(D8), 10,219–10,236, doi:10.1029/1999JD901122.
- Bruegge, C. J., N. L. Chrien, R. R. Ando, D. J. Diner, W. A. Abdou, M. C. Helmlinger, S. H. Pilorz, and K. J. Thome (2002), Early validation of the Multiangle Imaging Spectroradiometer (MISR) radiometric scale, *IEEE Trans. Geosci. Remote Sens.*, *40*(7), 1477–1492, doi:10.1109/TGRS.2002.801583.
- Burrows, J. P., et al. (1999), The Global Ozone Monitoring Experiment (GOME): Mission concept and first scientific results, *J. Atmos. Sci.*, *56*(2), 151–175, doi:10.1175/1520-0469(1999)056<0151:TGOMEG>2.0.CO;2.
- Diner, D. J., et al. (1998), Multiangle Imaging Spectroradiometer (MISR) instrument description and experiment overview, *IEEE Trans. Geosci. Remote Sens.*, *36*(4), 1072–1087, doi:10.1109/36.700992.
- Dong, X., et al. (2008), Using observations of deep convective systems to constrain atmospheric column absorption of solar radiation in the optically thick limit, *J. Geophys. Res.*, *113*, D10206, doi:10.1029/2007JD009769.
- Fröhlich, C. (2006), Solar irradiance variability since 1978: Revision of the PMOD composite during solar cycle 21, *Space Sci. Rev.*, *125*, 53–65, doi:10.1007/s11214-006-9046-5.
- Grenfell, T. C., S. G. Warren, and P. C. Mullen (1994), Reflection of solar radiation by the Antarctic snow surface at ultraviolet, visible, and near-infrared wavelengths, *J. Geophys. Res.*, *99*(D9), 18,669–18,684, doi:10.1029/94JD01484.
- Halthore, R. N., et al. (2005), Intercomparison of shortwave radiative transfer codes and measurements, *J. Geophys. Res.*, *110*, D11206, doi:10.1029/2004JD005293.
- Hansen, J. E. (1969), Exact and approximate solutions for multiple scattering by cloudy and hazy planetary atmospheres, *J. Atmos. Sci.*, *26*(3), 478–487, doi:10.1175/1520-0469(1969)026<0478:EAASF>2.0.CO;2.
- Hudson, S. R., and S. G. Warren (2007), An explanation for the effect of clouds over snow on the top-of-atmosphere bidirectional reflectance, *J. Geophys. Res.*, *112*, D19202, doi:10.1029/2007JD008541.
- Hudson, S. R., S. G. Warren, R. E. Brandt, T. C. Grenfell, and D. Six (2006), Spectral bidirectional reflectance of Antarctic snow: Measurements and parameterization, *J. Geophys. Res.*, *111*, D18106, doi:10.1029/2006JD007290.
- Hudson, S. R., S. Kato, and S. G. Warren (2010), Evaluating CERES angular distribution models for snow using surface reflectance observations from the East Antarctic Plateau, *J. Geophys. Res.*, *115*, D03101, doi:10.1029/2009JD012624.
- Kato, S., and N. G. Loeb (2005), Top-of-atmosphere shortwave broadband observed radiance and estimated irradiance over polar regions from Clouds and the Earth's Radiant Energy System (CERES) instruments on Terra, *J. Geophys. Res.*, *110*, D07202, doi:10.1029/2004JD005308.
- Kuhn, M., L. S. Kundla, and L. A. Stroschein (1977), The radiation budget at Plateau Station, Antarctica, 1966–1967, in *Meteorological Studies at Plateau Station, Antarctica*, edited by J. A. Businger, pp. 41–73, AGU, Washington, D. C.
- Lean, J., G. Rottman, J. Harder, and G. Kopp (2005), SORCE contributions to new understanding of global change and solar variability, *Sol. Phys.*, *230*, 27–53, doi:10.1007/s11207-005-1527-2.
- Loeb, N. G. (1997), In-flight calibration of NOAA AVHRR visible and near-IR bands over Greenland and Antarctica, *Int. J. Remote Sens.*, *18*(3), 477–490, doi:10.1080/014311697218908.
- Loeb, N. G., K. J. Priestley, D. P. Kratz, E. B. Geier, R. N. Green, B. A. Wielicki, P. O'Rawe Hinton, and S. K. Nolan (2001), Determination of unfiltered radiances from the Clouds and the Earth's Radiant Energy System instrument, *J. Appl. Meteorol.*, *40*, 822–835, doi:10.1175/1520-0450(2001)040<0822:DOURFT>2.0.CO;2.
- Masonis, S. J., and S. G. Warren (2001), Gain of the AVHRR visible channel as tracked using bidirectional reflectance of Antarctic and Greenland snow, *Int. J. Remote Sens.*, *22*(8), 1495–1520, doi:10.1080/01431160121039.
- Matthews, G., K. Priestley, P. Spence, D. Cooper, and D. Walikainen (2005), Compensation for spectral darkening of short wave optics occurring on the Clouds and the Earth's Radiant Energy System, in *Earth Observing Systems X, Proc. SPIE*, 5882, 588212, doi:10.1117/12.618972.
- McClatchey, R. A., R. W. Fenn, J. E. A. Selby, F. E. Volz, and J. S. Garing (1972), *Optical Properties of the Atmosphere (Third Edition)*, *Environmental Research Papers*, 411, Air Force Cambridge Res. Lab., Bedford, Mass.
- Pirazzini, R. (2004), Surface albedo measurements over Antarctic sites in summer, *J. Geophys. Res.*, *109*, D20118, doi:10.1029/2004JD004617.

- Rottman, G. (2005), The SORCE mission, *Sol. Phys.*, 230, 7–25, doi:10.1007/s11207-005-8112-6.
- Warren, S. G. (1984), Optical constants of ice from the ultraviolet to the microwave, *Appl. Opt.*, 23(8), 1206–1225.
- Warren, S. G., and R. E. Brandt (2008), Optical constants of ice from the ultraviolet to the microwave: A revised compilation, *J. Geophys. Res.*, 113, D14220, doi:10.1029/2007JD009744.
- Warren, S. G., R. E. Brandt, and P. O’Rawe Hinton (1998), Effect of surface roughness on bidirectional reflectance of Antarctic snow, *J. Geophys. Res.*, 103(E11), 25,789–25,807, doi:10.1029/98JE01898.
- Warren, S. G., R. E. Brandt, and T. C. Grenfell (2006), Visible and near-ultraviolet absorption spectrum of ice from transmission of solar radiation into snow, *Appl. Opt.*, 45(21), 5320–5334, doi:10.1364/AO.45.005320.
- Woods, T. N., P. C. Chamberlin, J. W. Harder, R. A. Hock, M. Snow, F. G. Eparvier, J. Fontenla, W. E. McClintock, and E. C. Richard (2009), Solar irradiance reference spectra (SIRS) for the 2008 Whole Heliosphere Interval (WHI), *Geophys. Res. Lett.*, 36, L01101, doi:10.1029/2008GL036373.
- 
- S. R. Hudson, Norwegian Polar Institute, Polar Environmental Centre, N-9296 Tromsø, Norway. (hudson@npolar.no)
- S. Kato, Climate Science Branch, NASA Langley Research Center, Mail Stop 420, Hampton, VA 23681-2199, USA. (seiji.kato@nasa.gov)
- S. G. Warren, Department of Atmospheric Sciences, University of Washington, Box 351640, Seattle, WA 98195-1640, USA. (sgw@atmos.washington.edu)